Food & Function

PAPER

View Article Online
View Journal | View Issue

Cite this: *Food Funct.*, 2016, **7**, 79

Wild Roman chamomile extracts and phenolic compounds: enzymatic assays and molecular modelling studies with VEGFR-2 tyrosine kinase

Rafaela Guimarães,[a,b] Ricardo C. Calhelha,[a,b] Hugo J. C. Froufe,[a] Rui M. V. Abreu,[a] Ana Maria Carvalho,[a] Maria João, R. P. Queiroz[b] and Isabel C. F. R. Ferreira*[a]

Received 21st May 2015,
Accepted 21st September 2015

DOI: 10.1039/c5fo00586h

www.rsc.org/foodfunction

Angiogenesis is a process by which new blood vessels are formed from the pre-existing vasculature, and it is a key process that leads to tumour development. Some studies have recognized phenolic compounds as chemopreventive agents; flavonoids, in particular, seem to suppress the growth of tumor cells modifying the cell cycle. Herein, the antiangiogenic activity of Roman chamomile (*Chamaemelum nobile* L.) extracts (methanolic extract and infusion) and the main phenolic compounds present (apigenin, apigenin-7-*O*-glucoside, caffeic acid, chlorogenic acid, luteolin, and luteolin-7-*O*-glucoside) was evaluated through enzymatic assays using the tyrosine kinase intracellular domain of the Vascular Endothelium Growth Factor Receptor-2 (VEGFR-2), which is a transmembrane receptor expressed fundamentally in endothelial cells involved in angiogenesis, and molecular modelling studies. The methanolic extract showed a lower IC_{50} value (concentration that provided 50% of VEGFR-2 inhibition) than the infusion, 269 and 301 μg mL^{-1}, respectively. Regarding phenolic compounds, luteolin and apigenin showed the highest capacity to inhibit the phosphorylation of VEGFR-2, leading us to believe that these compounds are involved in the activity revealed by the methanolic extract.

1. Introduction

Angiogenesis is a process by which new blood vessels are formed from the pre-existing vasculature, developing a hemovascular network.[1] It is tightly controlled by a balance of angiogenesis factors and inhibitors, occurring in the embryonic development, wound healing and the female reproductive cycle. Angiogenic diseases result from new blood vessels growing either excessively (*e.g.* cancer, diabetic retinopathy and psoriasis) or insufficiently (*e.g.* chronic wounds and ischaemic heart disease).[1,2]

During angiogenesis, endothelial cells degrade the basement membrane, migrate into the surrounding intercellular matrix, proliferate to form new blood vessels, and differentiate into contiguous tubular sprouts, which subsequently form functional capillary loops. Such cellular events are mediated by various intracellular signal transduction pathways.[3,4] Angiogenesis happens in the body all the time. It occurs through a so-called angiogenesis "cascade" which involves a series of biochemical steps by which cells make and secrete molecules that initiate the growth of capillaries. After the process is over, certain other molecular "factors" turn off the angiogenesis process. Cancer cells use this normal process for another purpose, creating an imbalance of angiogenesis activators that overrides the inhibitors and gives the nearby tumour ready access to a blood supply.[5] This explains why angiogenesis is essential for the growth, progression, and metastasis of solid tumours.[6]

In the mentioned pathophysiological processes, excessive angiogenesis occurs when diseased cells produce abnormally large amounts of angiogenesis factors [*e.g.* vascular endothelial growth factor (VEGF), fibroblast growth factor (FGF)-2 and hepatocyte growth factor], overcoming the effects of natural angiogenesis inhibitors (*e.g.* angiostatin, endostatin and thrombospondin).[1]

VEGF is a secreted growth factor by tumor cells that plays a critical role in angiogenesis; low oxygen tension dramatically induces the expression of this major angiogenic factor.[7] Its biological effects are mediated by two receptor tyrosine kinases namely VEGFR-1 (fms-like tyrosine kinase, Flt-1) and VEGFR-2 (kinase-insert domain-containing receptor, KDR), which differ considerably in their signalling characteristics.[8,9] Although increasing evidence indicates that angiogenesis is a highly sophisticated and coordinated process, the activation of

[a]*Centro de Investigação de Montanha, Escola Superior Agrária, Campus de Santa Apolónia, apartado 1172, 5301-854 Bragança, Portugal. E-mail: iferreira@ipb.pt; Fax: +351-273-325405; Tel: +351-273-303219*
[b]*Centro de Química da Universidade do Minho, Campus de Gualtar, 4710-057 Braga, Portugal*

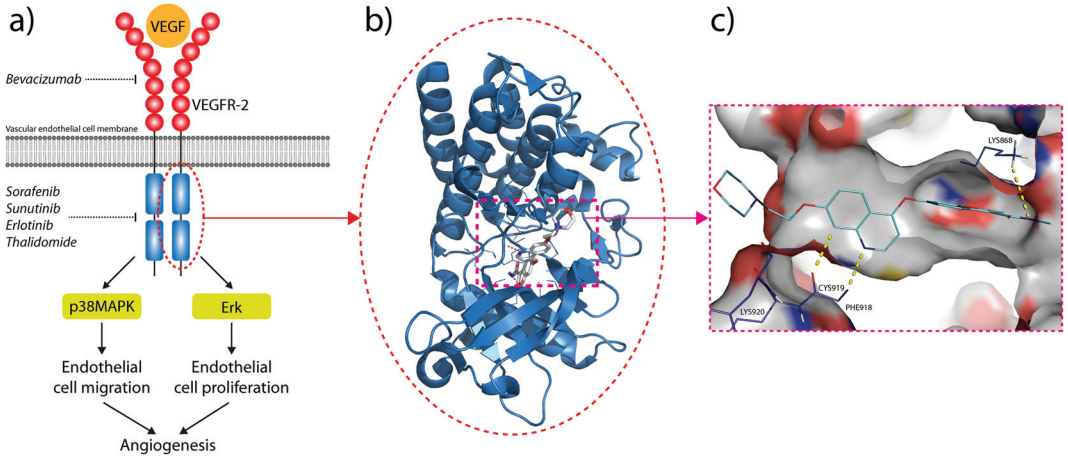

Fig. 1 (a) Main angiogenesis signaling pathways mediated by VEGFR-2; (b) X-ray crystal structure of the VEGFR-2 intracellular tyrosine kinase domain (PDB: 2XIR), co-crystallized with a TKI; (c) detailed representation of the ATP binding pocket and adjacent binding pockets showing the main interactions between VEGF-2 and the TKI (PDB: 2XIR).

the VEGF/VEGFR pathway remains the key modulator of angiogenesis.[10] Furthermore, VEGF is the leading angiogenic factor involved in tumoral angiogenesis.[7,9]

Of the primary receptors, VEGFR-2 is thought to mediate the majority of tumor angiogenic effects (Fig. 1a). Current clinical treatments against tumor antiangiogenesis that target VEGFR-2 include: monoclonal antibodies (*e.g.* bevacizumab) that target the VEGFR-2 extracellular VEGF binding domain and small tyrosine kinase inhibitors (TKIs) that target the VEGFR-2 intracellular tyrosine kinase domain (Fig. 1b). TKIs act by binding to the ATP binding pocket and to the adjacent pockets thus preventing the phosphorylation of this intracellular domain (*e.g.*, sunitinib, sorafenib, ZD6474, erlotinib or thalidomide) and blocking the angiogenic signaling pathway (Fig. 1c), lowering blood tumoral irrigation, and improving chemotherapy distribution.[9]

Several polyphenolic compounds are recognized as cancer chemopreventive agents. Flavonoids are especially well known to suppress tumor cell growth *via* cell-cycle arrest and by the induction of apoptosis in several tumor cell lines.[11,12] Moreover, flavonoids namely genistein inhibit endothelial cell cultures on collagen gels.[13] The antiangiogenic effect of apigenin on tumor cells was also reported and related to a reduction in the expression of VEGF.[12]

Other plant-derived anticancer drugs (*e.g.* Taxol®, camptothecin and combretastatin) proved to be antiangiogenic. In traditional Chinese medicine, many herbs are used in the treatment of angiogenic diseases such as chronic wounds and rheumatoid arthritis.[1] Furthermore, it has been reported that drinking green tea could inhibit VEGF-induced angiogenesis *in vivo*.[5]

In a previous study, we reported the antitumor activity of Roman chamomile (*Chamaemelum nobile* L.) methanolic extract and infusion in five different human tumour cells (non-small cell lung cancer, breast, colon, cervical and hepatocellular carcinomas). Furthermore, flavonoids such as flavonols and flavones, phenolic acids and derivatives were found in this wild herb.[14] In the present work, the antiangiogenic activity of Roman chamomile (*Chamaemelum nobile* L.) extracts (methanolic extract and infusion) and main phenolic compounds (apigenin, apigenin-7-*O*-glucoside, caffeic acid, chlorogenic acid, luteolin, and luteolin-7-*O*-glucoside) were evaluated through enzymatic assays using the tyrosine kinase intracellular domain of VEGFR-2. To better understand the inhibition phosphorylation mechanism of the tyrosine kinase receptor by luteolin, apigenin and apigenin-7-*O*-glucoside, docking studies were performed.

2. Materials and methods

2.1 Biological material and sample preparation

C. nobile was gathered during the flowering season (June–July 2010) from wild populations located in grasslands in Bragança (Trás-os-Montes, Northeastern Portugal). Samples consist of pieces of about 8 cm, corresponding to terminal soft leafy stems and inflorescences with flowers fully open and functional, picked up in plants randomly selected in a meadow of about a hectare. The plant material was put together in a single sample for analysis. Voucher specimens are deposited in the Herbarium of the Escola Superior Agrária de Bragança (BRESA). The sample was lyophilized (FreeZone 4.5, Labconco, Kansas, USA), reduced to a fine dried powder (20 mesh) and mixed to obtain a homogenate sample.

A methanolic extract was prepared from the lyophilized plant material. The sample (1 g) was extracted by stirring with 25 mL of methanol (25 °C at 150 rpm) for 1 h and subsequently filtered through Whatman No. 4 paper. The residue was then extracted with 25 mL of methanol (25 °C at 150 rpm) for 1 h. The combined methanolic extracts were evaporated at 40 °C (rotary evaporator Büchi R-210) to dryness and re-dissolved in DMSO to a final concentration of 400 μg mL^{-1}.

An infusion was also prepared from the lyophilized plant material. The sample (1 g) was added to 200 mL of boiling distilled water and left to stand at room temperature for 5 min, and then filtered under reduced pressure. The obtained infusion was frozen, lyophilized and re-dissolved in DMSO to a final concentration of 400 μg mL^{-1}.

2.2. Phenolic compounds

Apigenin, apigenin-7-*O*-glucoside, caffeic acid, chlorogenic acid, luteolin, and luteolin-7-*O*-glucoside were from Extrasynthese (Genay, France). Each phenolic compound was dissolved in DMSO to a final concentration of 40 μg mL^{-1}.

2.3. VEGFR-2 enzymatic inhibition assay

C. nobile methanolic extract and infusion, and the pure phenolic compounds were assessed for VEGFR-2 inhibition activity using the Z′-LYTE-Tyr1 Peptide assay kit (Invitrogen, Cat. PV3190) according to the procedures recommended by the manufacturer.[15] Briefly, assays were performed in a total of 20 μL in 384-well plates using fluorescence resonance energy transfer technology. A Tyr1 substrate (coumarin-fluorescein double-labeled peptide) at 1 μM was incubated for 1 h with 4 μg mL^{-1} VEGFR-2, 50 μM ATP and the *C. nobile* methanolic extract/infusion (400 at 6.25 μg mL^{-1}) or the pure phenolic compounds (40 at 0.04 μg mL^{-1}) at room temperature in 50 mM Hepes/NaOH (pH 7.5), 10 mM $MgCl_2$, 2 mM $MnCl_2$, 2.5 mM DTT, 0.1 mM orthovanadate, and 0.01% bovine serum albumin. The wells were incubated at 25 °C for 1 h and 5 μL development reagents were added to each well. After a second incubation of 1 h a stop reagent was added to each well. Using a Biotek FLX800 micro-plate the fluorescence was read at 445 nm and 520 nm (excitation 400 nm), and Gen5™ Software was used for data analysis. Genistein (Extrasynthese, Genay, France) was used as positive control.

The assays were performed in triplicate and the results were expressed as mean values ± standard deviation (SD). The results were analyzed using a Student's *t*-test with $\alpha = 0.05$, to determine the significant difference among the two extracts. For the phenolic compounds, the analysis was performed using one-way analysis of variance (ANOVA) followed by Tukey's HSD test with $\alpha = 0.05$. These treatments were carried out using the SPSS v. 22.0 program.

2.4 Docking simulations using AutoDockVina

The 2D structure of the compounds apigenin, apigenin-7-*O*-glucoside, luteolin and luteolin-7-*O*-glucoside was constructed using the ACD/ChemSketch Freeware 12.0 software. Open Babel[16] was used to convert compounds from 2D to 3D and they were saved in the pdb format.

A VEGFR-2 crystal structure (PDB: 2XIR) was extracted from the Protein Data Bank (PDB) (http://www.rcsb.org). The co-crystallized ligand was extracted from the PDB file, and AutoDockTools[17] was used to assign polar hydrogens and Gasteiger charges to the compounds and VEGFR-2 protein. All structures were saved in the PDBQT file format required to use AutoDockVina.[18] AutodockVina was used to perform docking in an area of 30 Å × 30 Å × 30 Å, centered on the co-crystallized ligand. The docking simulations were performed on a cluster of 6 AMD Opteron 6128 8 core 2.0 GHz by using MOLA software.[19] All figures with structure representations were prepared using PyMOL (The PyMOL Molecular Graphics System, Version 1.3, Schrödinger, LLC). Available at: (http://www.pymol.org/). Accessed on 03 September, 2012.

2.5 Molecular dynamics simulation

The protein preparation wizard from Maestro (Schrodinger, LLC, Portland, OR) was used to prepare ligand/VEGFR-2 complexes and then used to perform explicit solvent molecular dynamics (MD) simulations. The parallelized Desmond Molecular Dynamics System v2.2 (D. E. Shaw Research, New York, NY) and associated analysis tools, available within the Schrodinger suite (Schrodinger, LLC, Portland, OR), were used for this purpose. The protocol used was described by Mukherjee *et al.*[20]

3. Results and discussion

According to previous studies of the authors, Roman chamomile is an equilibrated valuable species rich in carbohydrates and proteins, and poor in fat, providing tocopherols, carotenoids and essential fatty acids (C18:2n6 and C18:3n3). Moreover, the herb and its infusion are a source of phenolic compounds and organic acids with high bioactive potential.[14] Herein, methanolic extract, infusion and phenolic compounds of Roman chamomile were evaluated for their ability to interact with the VEGFR-2 kinase domain, using an enzymatic (fluorescence resonance energy transfer) FRET-based assay. The results are shown in Table 1.

The methanolic extract showed a lower IC_{50} value than the infusion, 269 and 301 μg mL^{-1}, respectively. These results are in agreement with the higher phenolic compound amount, antioxidant and antitumor activities also previously reported for the methanolic extract.[14]

Table 1 VEGFR-2 inhibition activity of *Chamaemelum nobile* extracts and phenolic compounds (mean ± SD)

Chamaemelum nobile	VEGFR-2 IC_{50}, μg mL^{-1}
Methanolic extract	269.26 ± 8.74
Infusion	301.09 ± 13.07
Student's *t* test; *p*-value	<0.001
Phenolic compound	VEGFR-2 IC_{50}, μg mL^{-1}
Luteolin	$0.60 \pm 0.03^{c*}$
Apigenin	1.29 ± 0.07^{b}
Apigenin-7-*O*-glucoside	19.21 ± 1.58^{a}
Luteolin-7-*O*-glucoside	>40
Caffeic acid	>40
Chlorogenic acid	>40
Genistein	1.04 ± 0.06

IC_{50}-concentration that provided 50% of VEGFR-2 inhibition. *Different letters mean significant differences between compounds ($p < 0.05$).

Regarding individual molecules, apigenin, apigenin-7-*O*-glucoside, caffeic acid, chlorogenic acid, luteolin and luteolin-7-*O*-glucoside were chosen because these compounds were the ones used to quantify all the phenolic compounds identified in Roman chamomile.[14] Phenolic acids (caffeic and chlorogenic acids) and luteolin-7-*O*-glucoside did not show the VEGFR-2 inhibition activity (IC_{50} values higher than 40 μg mL^{-1}), whereas apigenin-7-*O*-glucoside showed VEGFR-2 inhibition activity with the IC_{50} value = 19.21 μg mL^{-1}. A drastic increase in the VEGFR-2 inhibition activity was observed for the corresponding aglycones (compounds without the glycosyl group) of the mentioned flavonoids: luteolin and apigenin (IC_{50} values = 0.60 and 1.29 μg mL^{-1}, respectively). The active concentrations, corresponding to the last IC_{50} values, are easily provided by the Roman chamomile infusion, which contains 8.42 μg mL^{-1} and 9.28 μg mL^{-1} of luteolin and apigenin derivatives (compounds with glycosyl groups: luteolin-7-*O*-glucoside and apigenin-7-*O*-glucoside), respectively (values calculated from the ones reported previously by the authors and taking into account the extraction yields).[14] It should be highlighted that the methanolic extract prepared from the herb would provide even higher amounts of those derivatives (21.31 and 13.50 μg mL^{-1}, respectively[14]).

The possible VEGFR-2 inhibition mechanism of luteolin, apigenin and apigenin-7-*O*-glucoside (Fig. 2) was predicted using docking tools. A careful analysis of the predicted docking poses showed that apigenin and luteolin probably interact with the VEGFR-2 ATP binding site with a similar binding pose, stabilized by three predicted hydrogen bonds (Fig. 3): one H-bond between the CYS919 backbone and the carbonyl group at position 3 of the benzopyrone moiety; a second H-bond between the CYS919 backbone and the hydroxyl group at position 5 of the benzopyrone moiety; and a third H-bond between the amino group of the LYS868 side chain and the hydroxyl group at position 4 of the benzene ring. The higher VEGFR-2 inhibition capacity of luteolin compared to apigenin can probably be explained by the better occupation of the ATP binding site, accomplished by the lutein extra hydroxyl group occupation of a small pocket located inside the structure shown in Fig. 3. Furthermore, comparing the docking poses of apigenin and apigenin-7-*O*-glucoside, it was possible to observe that the presence of the glucoside moiety shifts the compound slightly away from the ATP binding site. This shift probably weakens the described H-bonds, explaining the lower VEGFR-2 inhibition capacity of apigenin-7-*O*-glucoside.

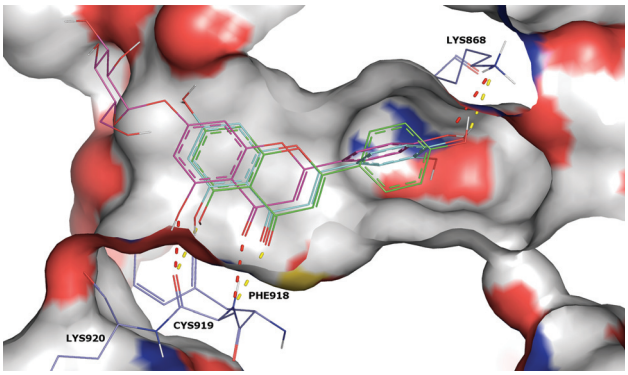

Fig. 3 Surface representation of the VEGFR-2 ATP binding site docked with apigenin (green line), luteolin (blue line) and apigenin-7-*O*-glucoside (magenta line). Apigenin and luteolin hydrogen bonds are represented as yellow dashes, and apigenin-7-*O*-glucoside hydrogen bonds as red dashes.

Moreover, the inability of AutodockVina to predict the binding pose of luteolin-7-*O*-glucoside similar to luteolin, apigenin and apigenin-7-*O*-glucoside seems to indicate that luteolin-7-*O*-glucoside probably cannot interact with the ATP binding site. This was experimentally proved by the high IC_{50} value obtained in the enzymatic assay (>100 μM).

MD (Molecular Dynamics) simulations were performed using the most active compounds, luteolin and apigenin, to verify whether both the predicted docking poses remain stable in a more physiologically relevant setting. The docking poses of both complexes were the starting points for 5 ns MD simulations, and the overall stability of each MD simulation was evaluated by plotting the receptor backbone (VEGFR-2) and ligands' RMSD (Root Mean Square Deviation) as a function of time (Fig. 4).

After small adjustments in the first ns of the MD simulation, both apigenin and luteolin structures remained stable during the MD simulation with an average RMSD of 0.37 and 0.57 Å, respectively (Fig. 4). This is an indication that the predicted docking pose is reliable and is probably close to the experimental VEGFR-2 binding pose. In both MD simulations, the RMSD values for the VEGFR-2 backbone structure were also analyzed and it was observed that, after a normal adjustment of around 2 ns, the RMSD values also remained stable during rest of the MD simulation. This is the expected MD simulation behavior of the protein backbone indicating that the VEGFR-2 structure used is suitable for this type of molecular modeling study.

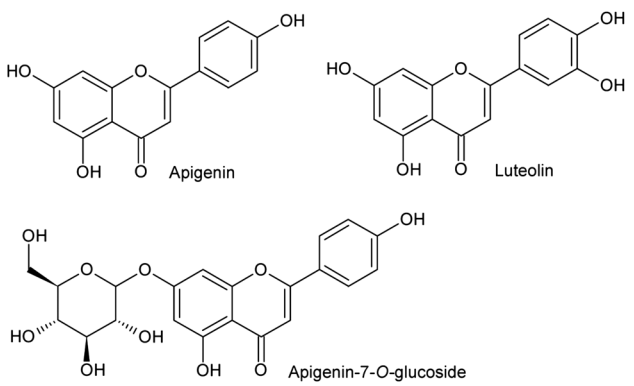

Fig. 2 Chemical structures of luteolin, apigenin and apigenin-7-*O*-glucoside.

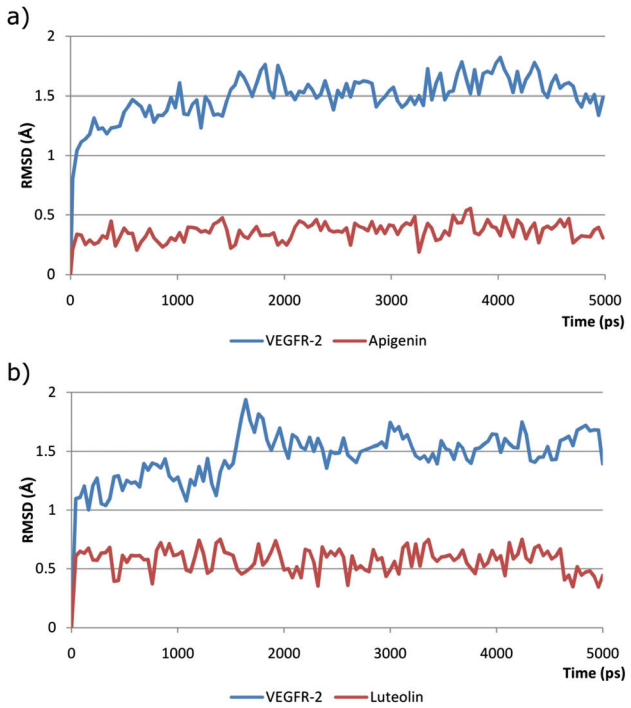

Fig. 4 RMSD values obtained during the 5 ns MD simulation timeframe for: (a) VEGFR-2/apigenin and (b) VEGFR-2/luteolin complexes.

In general the MD simulations performed gave us further assurance that the predicted docking pose probably corresponds closely to the experimental binding pose although this can only be completely established by the elucidation of the VEGFR-2/apigenin or VEGFR2/luteolin complex structures, usually performed by X-ray crystallography.

The antiangiogenic effect of apigenin on tumor cells has already been reported but related to the reduction in the expression of VEGF[12] and not to the inhibition of VEGFR activity, so it is demonstrated in the present work. Regarding luteolin, as far as we know this is the first report on antiangiogenic activity, and only its anticarcinogenic effects mainly by induction of apoptosis and cell cycle arrest by the action on critical molecular targets for cell survival such as p53, p21, cyclin dependent kinases and caspases in liver[21] and non-small cell lung[22] cancer cells are reported.

Acknowledgements

The authors are grateful to strategic projects PEst-OE/AGR/UI0690/2014 and PEst-C/QUI/UI0686/2013–2014 for financial support to the research centres. R. Guimarães, and R. Calhelha thank FCT, POPH-QREN and FSE for their grants (SFRH/BD/78307/2011 and SFRH/BPD/68344/2010).

References

1 T.-P. Fan, J.-C. Yeh, K. H. Leung, P. Y. K. Yue and R. N. S. Wong, *Trends Pharmacol. Sci.*, 2006, **27**, 297–309.
2 J. Folkman, *Nat. Med.*, 1995, **1**, 27–31.
3 H. K. Avraham, T. H. Lee, Y. Koh, T. A. Kim, S. Jiang, M. Sussman, A. M. Samarel and S. Avraham, *J. Biol. Chem.*, 2003, **278**, 36661–36668.
4 J. Jeon, J. Lee, C. Kim, Y. An and C. Choi, *Microvasc. Res.*, 2010, **80**, 303–309.
5 T. K. Maiti, J. Chatterjee and S. Dasgupta, *Biochem. Biophys. Res. Commun.*, 2003, **308**, 64–67.
6 L. A. Liotta, P. S. Steeg and W. G. Stetler-Stevenson, *Cell*, 1991, **64**, 327–336.
7 J. A. Forsythe, B. H. Jiang, N. V. Iyer, F. Agani, S. W. Leung, R. D. Koos and G. L. Semenza, *Mol. Cell. Biol.*, 1996, **16**, 4604–4613.
8 Y. Huang, X. Chen, K. M. Dikov, S. V. Novitskiy, C. A. Mosse, L. Yang and D. P. Carbone, *Blood*, 2007, **110**, 624–631.
9 J. F. Morère, J. M. Brechot and R. Etessami, *Targeted Oncol.*, 2006, **1**, 215–219.
10 C.-M. Lin, H. Chang, Y.-H. Chen, S. Y. Li, I.-H. Wu and J.-H. Chiu, *Int. Immunopharmacol.*, 2006, **6**, 1690–1698.
11 C. Kandaswami, L. T. Lee, P. P. Lee, J. J. Hwang, F. C. Ke, Y. T. Huang and M. T. Lee, *in Vivo*, 2005, **19**, 895–909.
12 M. Osada, S. Imaoka and Y. Funae, *FEBS Lett.*, 2004, **575**, 59–63.
13 T. Fotsis, M. Pepper, H. Adlercreutz, G. Fleischamann, T. Hase, R. Montesano and L. Scheweigerer, *Proc. Natl. Acad. Sci. U. S. A.*, 1993, **90**, 2690–2694.
14 R. Guimarães, L. Barros, M. Dueñas, R. C. Calhelha, A. M. Carvalho, C. Santos-Buelga, M. J. R. P. Queiroz and I. C. F. R. Ferreira, *Food Chem.*, 2013, **136**, 718–725.
15 P. Soares, R. Costa, H. J. C. Froufe, R. C. Calhelha, D. Peixoto, I. C. F. R. Ferreira, R. M. V. Abreu, R. Soares and M. J. R. P. Queiroz, *BioMed Res. Int.*, 2013, 154856.
16 N. M. O'Boyle1, M. Banck and C. A. James, http://www.jcheminf.com/content/3/1/33/-ins3; C. Morley, T. Vandermeersch and G. R. Hutchison, *J. Cheminf.*, 2011, **3**, 33.
17 M. F. Sanner, *Structure*, 2005, **13**, 447–462.
18 O. Trott and A. J. Olson, *J. Comput. Chem.*, 2010, **31**, 455–461.
19 R. M. Abreu, H. J. Froufe, M. J. R. P. Queiroz and I. C. F. R. Ferreira, *J Cheminf.*, 2010, **2**, 10.
20 P. Mukherjee, F. Shah, P. Desai and M. Avery, *J. Chem. Inf. Model.*, 2011, **51**, 1376–1392.
21 D. Stagos, G. D. Amoutzias, A. Matakos, A. Spyrou, A. M. Tsatsakis and D. Kouretas, *Food Chem. Toxicol.*, 2012, **50**, 2155–2170.
22 X. Cai, T. Ye, C. Liu, W. Lu, M. Lu, J. Zhang, M. Wang and P. Cao, *Toxicol. in Vitro*, 2011, **25**, 1385–1391.